THE ADVANCED X-RAY ASTROPHYSICS FACILITY (AXAF)

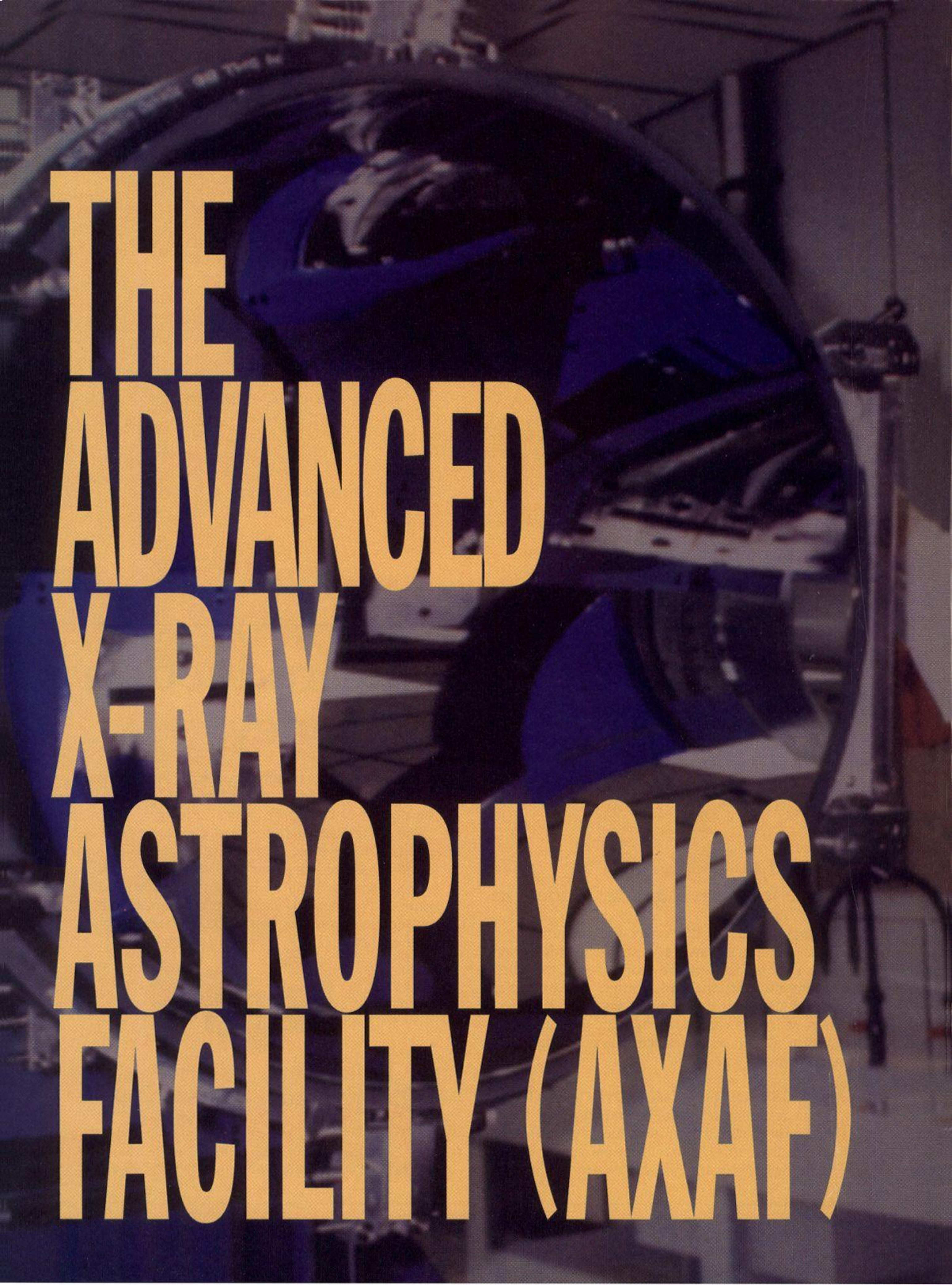

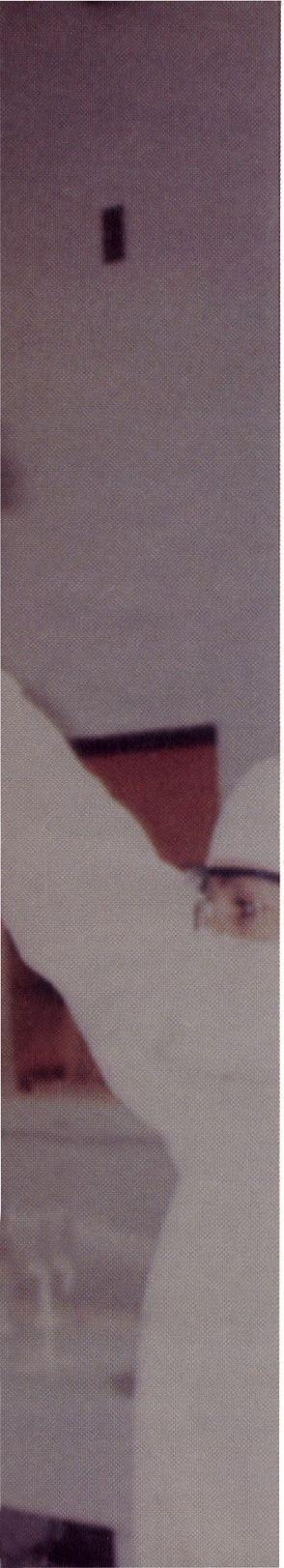

By Martin C. Weisskopf
and Leon Van Speybroeck

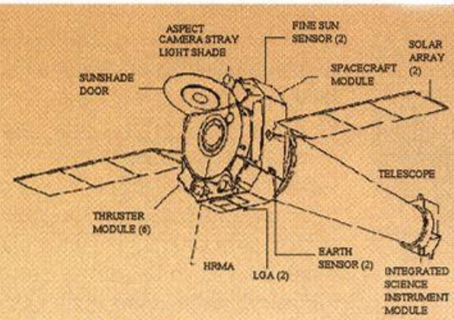

Figure 1. Major elements of the AXAF observatory.

Snapshot: The authors discuss the optics and instruments of NASA's nearly completed x-ray observatory.

Significant advances in science always seem to take place when the state of the art in instrumentation improves. NASA's next Great Observatory, the Advanced x-ray Astrophysics Facility (AXAF), represents such an advance. AXAF is an observatory designed to study the x-ray emission from all categories of astronomical objects, from normal stars to quasars. Major elements of the observatory—the optics and scientific instruments—are nearing completion this year in preparation for calibration and eventual launch in late 1998.

AXAF has broad scientific objectives and an outstanding capability to provide high-resolution (<1 arcsec) images, spectrometric imaging, and high-resolution dispersive spectroscopy over the energy bandwidth from 0.1–10 keV.

1047-6938/96/4/0016/07-$0010.00

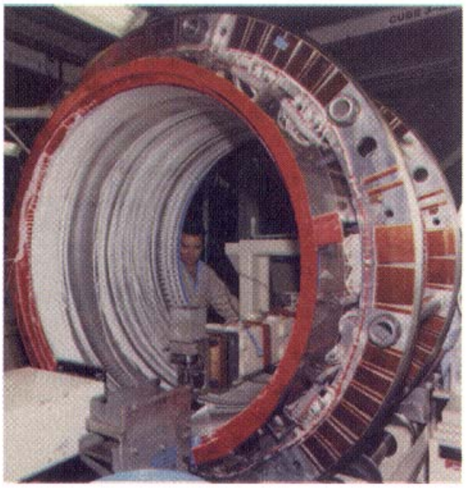

Figure 2. The largest AXAF paraboloid is shown being ground under computer control at Hughes Danbury Optical Systems. The aluminum support rings were used during grinding and polishing, but were removed during metrology.

NASA's Marshall Space Flight Center manages the AXAF project with scientific and technical support from the Smithsonian Astrophysical Observatory (SAO). TRW's Space and Electronics Group is the prime contractor and provides overall systems engineering and integration. Major subcontracts that relate directly to the optics include Hughes Danbury Optical Systems (HDOS), which built the x-ray optics discussed below; Optical Coating Laboratory, which coated the optics with sputtered iridium; and Eastman Kodak Co., responsible for mounting and aligning the optics and providing the optical bench. Other optical systems on AXAF include a CCD-based visible-light imaging aspect camera to record star images and provide data for reconstructing the direction in which the Observatory is pointed. Ball Aerospace & Technologies is responsible for the aspect camera system. The scientific instruments comprise two sets of objective transmission gratings, which can be inserted just behind the x-ray optics, and two sets of focal-plane imaging detectors, which can be positioned at the end of the 10-m focal length.

The fully deployed AXAF, shown schematically in Figure 1 (page 17), is 13.8-m (45.3-ft) long, has a 19.5-m (64-ft) solar array wingspan, and has a 4,500-kg (5-ton) on-orbit mass. AXAF will be placed in a highly elliptical orbit with a 140,000-km apogee and a 10,000-km perigee by means of the space shuttle and Boeing's inertial upper stage.

The x-ray optics

The heart of the observatory is the x-ray telescope. The characteristics of these optics largely derive from the fact that x-rays reflect efficiently only if the grazing angle between the incident ray and the reflecting surface is less than the critical angle. This angle, typically of order one degree, is approximately $10^{-2}(2\rho)^{1/2}/E$, where ρ is the density in g/cm^{-3} and E is the photon energy in keV, so higher energy telescopes must have smaller grazing angles. The x-ray optical elements for AXAF and similar telescopes resemble shallow angle cones, and at least two reflections are required to provide good imaging over a useful field of view; the first AXAF surface is a paraboloid and the second a hyperboloid. The collecting area can be increased by nesting concentric mirror pairs, all having the same focal plane. The wall thickness of the inner elements limits the number of pairs, and designs have tended to fall into two classes—those with relatively thick walls to achieve stability, and hence angular resolution, at the expense of collecting area, and those with very thin walls to maximize collecting area, thus sacrificing angular resolution. The Einstein (1978), German ROSAT (1990), and AXAF (1998) mirrors are examples of high-resolution designs, while the Japanese ASCA (1993) and European XMM (1999) mirrors are examples of emphasis on large collecting area.

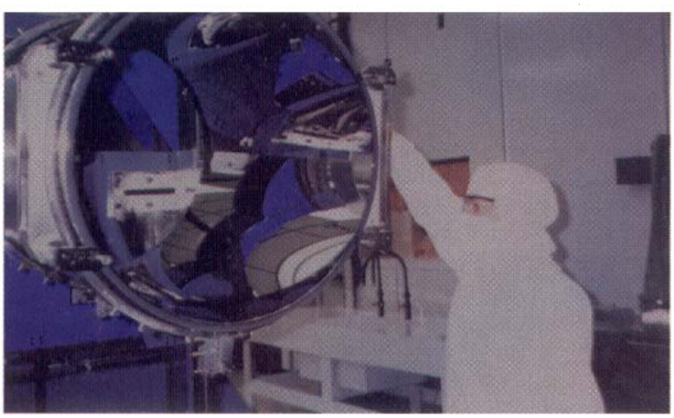

Figure 3. The smallest AXAF paraboloid is shown in its handling fixture after being coated with iridium at Optical Coating Laboratories Inc.

Figure 4. The mirror support structure designed by the Eastman Kodak Co. supports the AXAF mirror elements near their centers with radially compliant flexures attached to carbon fiber composite support sleeves. The inner support cylinder and some of the thermal control heaters also can be seen.

The final mirror design for AXAF includes 8 optical elements comprising four paraboloid/hyperboloid pairs that have a common 10-m focal length, element lengths of about 0.83 m, diameters of approximately 0.63, 0.85, 0.97, and 1.2 m, and wall thickness between about 16 mm for the smaller elements and 24 mm for the outer ones. Zerodur from Schott was selected for the optical element material because of its low coefficient of thermal expansion and previously demonstrated capability of permitting very smooth polished surfaces.

HDOS manufactured the mirror elements. The major fabrication phases included coarse and fine grinding, polishing, and final smoothing. The grinding and polishing operations were done with relatively small tools under computer control. The cycle was iterative; a mirror element was measured to yield an error map, appropriate small tools were selected to reduce the errors, and a polishing control file for the next cycle was generated that caused more material removal in the high areas. The residual errors were smaller than the original, so the process converged to the required accuracies.

HDOS used three principal metrology instruments for fabrication and final acceptance data. Axial figure errors at fixed azimuthal angles were measured in the Precision Metrology Station (PMS) by interferometric measurement of the separation between the optical surface and a calibrated reference surface. A Circularity and Inner Diameter Station (CIDS) was used to determine the inner diameters and roundness errors near the ends of the mirrors. These instruments each included two pairs of opposed contacting radial probes, calibrated reference bars, positioning mechanisms, and a precise air bearing to permit rotation. The instruments were housed in environmentally controlled enclosures, and the mirror elements were carefully supported vertically to achieve the required accuracy. The micro-phase measuring interferometer (MPMI), an adaptation of a WYKO instrument, was used to obtain high-frequency roughness measurements for small samples of the mirror surfaces.

The x-ray performance is more sensitive to high-frequency than to low-frequency errors, and more sensitive to axial than to circumferential errors, and this is reflected in the accuracies of the instruments; about 0.5, 20, and 200-Å-rms for the MPMI, PMS, and CIDS, respectively. Numerous cross-checks, such as comparisons with data from other (but less accurate) instruments and different optical orientations, were performed to avoid serious undetected systematic errors. The data reduction also was a substantial effort: the final data set, including both raw and processed data, consists of more than 40,000 computer files.

The PMS axial data and CIDS circumferential data were combined to yield low frequency surface error maps. These errors were reduced to an average of 50-Å-rms for the axial component by computer controlled polishing with small tools. This typically required four grinding and four polishing cycles per element, which is extremely rapid convergence by traditional optical shop experience. Figure 2 shows the largest optical element being ground at HDOS. The aluminum rings visible in the photo provided support to the optics during the abrasive material removal process, and were removed during measurements so that an essentially stress free shape could be determined. The heater elements on the rings were used to effect glass insertion or removal by differential expansion of the glass and support structure. The final polishing was performed with a large lap designed to reduce surface roughness without introducing unacceptable lower frequency figure errors. The resulting rms surface roughness over the central 90% of the elements varied between 1.85 and 3.44 Å in the 1–1,000 mm^{-1} band. This excellent surface smoothness enhances the encircled energy performance at higher energies. Fabrication of the eight AXAF optical elements was completed by HDOS approximately four months ahead of schedule; the expected performance exceeds the contractual specifications and goals at essentially all energies.

The mirror elements then were coated at Optical Coating Laboratories Inc. (OCLI) by sputtering with iridium over a chromium binding layer. OCLI performed verification runs with surrogates before each coating of flight glass. These surrogates included optical witness samples that were used to show that coating thickness would be uniform and that the surface smoothness would not be degraded. The x-ray reflectivities of the witness flats also were measured at SAO to ascertain that the expected densities were being achieved. Similar tests on witness samples coated at the same time as the flight optics indicate that the coatings should provide better than the specified performance and result in very little, if any, degradation of the surface smoothness. The last planned cleaning of the mirrors occurred at OCLI prior to coating, and stringent contamination controls were begun at that time. Figure 3 shows the smallest paraboloid in the OCLI handling fixture after being coated.

The final alignment and assembly of the mirror elements into the high resolution mirror assembly (HRMA) and other AXAF tasks are being done by Eastman Kodak Co. The completed mirror element support structure, designed by Kodak, is shown in Figure 4. Each mirror ele-

Fax Today! See page 62.

ment will be bonded near its mid-station to flexures previously attached to the carbon fiber composite mirror support sleeves. The four support sleeves and associated flexures for the paraboloids can be seen near the top of the photo, and those for the outer hyperboloid appear at the bottom. The inner support cylinder protruding at the top will support x-ray and thermal control apertures to be added later. Some of the thermal control heaters can be seen around the periphery of the structure. The flexures result in small radial forces on the mirrors, and therefore they reduce the support-induced axial slope errors, to which mirror performance is especially sensitive. The thin mirror shells are susceptible to a deformation mode in which both ends become oval, but with perpendicular major axes; support of the mirror elements near their centers minimizes the coupling of support errors into this mode. The final mirror alignment is performed with the optical axis vertical in a clean and environmentally controlled tower. The mirror elements are supported to approximate the gravity and strain-free state, are positioned mechanically and optically, and then are bonded to the flexures described above. The Bauer Associates optical instrument used for alignment generates a laser beam that passes through the x-ray optics, is reflected from an autocollimating flat, and returns through the x-ray optics to the instrument. The variation of the returned spot position with azimuth provides the information required to position the x-ray optical elements. After the x-ray elements are assembled, Kodak will add outer support cylinders, the remainder of the thermal control system, contamination covers, and components of the flight alignment system.

The HRMA will be taken to NASA's Marshall Space Flight Center for final x-ray calibration in the fall of 1996, and then to TRW for integration into the spacecraft. The largest mirror pair was x-ray-tested previously during the development program and showed a measured angular resolution of 0.22 arcsec (FWHM). The AXAF mirrors are the largest high-resolution x-ray optics ever made; their effective areas are shown as a function of energy in the left panel of Figure 5, along with those of their Einstein and ROSAT predecessors. The AXAF mirror areas are roughly a factor of four greater than the Einstein mirrors. The effective areas of AXAF and ROSAT are comparable at low energies because the somewhat smaller ROSAT mirrors have larger grazing angles; the smaller grazing angles of AXAF yield more throughput at higher energies. The fraction of the incident energy included in the core of the expected AXAF response to 1.49-keV X rays is shown as a function of image radius in the right panel of Figure 5. The methodology for predicting x-ray performance based on optical and mechanical metrology has been validated by excellent agreement between predictions and subsequent x-ray measurements taken for previous mirrors. The responses of the Einstein and ROSAT mirrors also are shown. The expected improvement within 0.5 arcsec is dramatic, although it is important to note that the ROSAT mirrors exceeded their specification and were well-matched to the principal detector for that mission. The excellent surface smoothness achieved for the AXAF and ROSAT mirrors results in a very modest variation of the performance as a function of energy; this will reduce the uncertainties that accrue from the use of calibration data to infer properties of sources with different spectra, and will improve the precision of the many quantitative experiments to be performed with the AXAF.

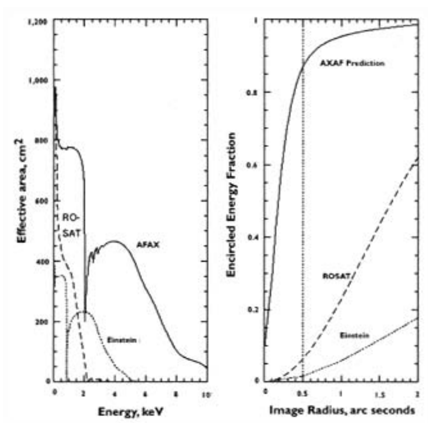

Figure 5. The effective areas of the AXAF, Einstein, and ROSAT mirrors are shown in the left panel as a function of energy. AXAF has significantly more area over a wider bandwidth than its predecessors. The expected fraction of the effective area included within the AXAF image as a function of radius is shown in the right panel for 1.49 keV x-rays. The observed responses for the Einstein and ROSAT mirrors also are shown, although neither was specified for these small angles and ROSAT exceeded its specification. The improvement within 0.5 arcsec is dramatic.

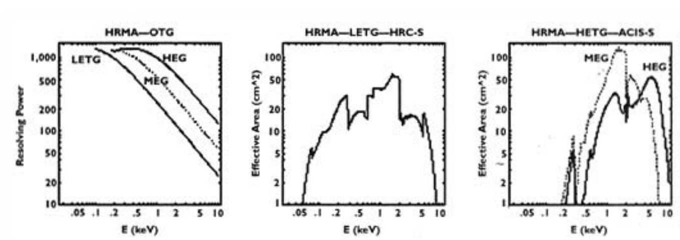

Figure 6. Expected spectroscopic performance of AXAF. Left panel shows the approximate resolving power. Central panel displays the effective area of the LETG spectrometer with the HRC-S readout. Right panel shows the effective area for the HETG spectrometers with the ACIS-S readout.

The scientific instruments

AXAF has two focal plane instruments—the high resolution camera (HRC) and the AXAF CCD imaging spectrometer (ACIS). Each of these, in turn, has two detectors: one for direct imaging of x-rays that pass through the optics and the other for imaging x-rays that are dispersed by the objective transmission gratings when the latter are commanded into place directly behind the HRMA. Each focal-plane detector operates in essentially photon counting mode and has very low internal background.

The HRC is produced at SAO with S. Murray the principal investigator. The imaging detector (HRC-I) is a large-format, 100-mm (4-in)-square microchannel plate coated with a cesium iodide photocathode to improve x-ray response. A conventional cross-grid charge detector reads out the photoinduced charge cloud and the electronics determine the arrival time (to 16-μs) and the position with a resolution of about 18 μm corresponding to 0.37 arcsec. The spectroscopy readout detector (HRC-S) is a 300 mm × 20 mm, three-section micro-channel plate. Sectioning allows the two outside sections to be tilted to conform more closely to the Rowland circle that includes the gratings.

The ACIS has two charge coupled-device (CCD) detector arrays—ACIS-I for high-resolution spectrometric imaging and ACIS-S for readout of the high-energy transmission gratings. G. Garmire (Pennsylvania State University) is the principal investigator. MIT's Center for Space Research, in collaboration with MIT Lincoln Laboratories, is developing the detector system and manufacturing the CCDs. Stray visible light is shielded by means of baffles and an optical blocking filter (1,500-Å aluminum on 1,000-Å Lexan). The imaging array is a 2 × 2 array of CCDs. The four CCDs tilt slightly toward the optics to conform more closely to the optical surface. Each CCD has 1024 × 1024 pixels of 24-μm (0.5-arcsec) size. This array is used primarily for spectrometric imaging. The ACIS spectroscopy readout has a 1 × 6 array tilted slightly to conform to the Rowland circle.

Both sets of objective transmission gratings consist of hundreds of individual coaligned facets mounted to supporting structures on four annuli (one for each of the four coaligned telescopes) to intercept the x-rays exiting from the HRMA. To optimize the energy resolution, the grating support structure holds the facets close to the Rowland toroid that intercepts the focal plane.

The low-energy transmission grating (LETG) will provide high-resolution spectroscopy at the lower end of the AXAF energy range. A. Brinkman (Space Research Organization of the Netherlands) is the principal investigator. The LETG is being developed in collaboration with the Max Planck Institut für Extraterrestische Physik (Germany). The LETG has 540 1.6-cm (0.63-in) diameter grating facets, three per grating module. Ultraviolet contact lithography is used to produce an integrated all-gold facet that is bonded to a stainless-steel facet ring. An individual facet has 0.43-μm-thick gold grating bars with 50% filling factor and 9920-Å period, resulting in 1.15 Å/mm dispersion. The HRC-S is the primary readout device for the LETG.

The high-energy transmission grating (HETG) will provide high-resolution spectroscopy at the higher end of the AXAF energy range. C. Canizares (Center for Space Research) is the principal investigator. This group is developing the instrument in collaboration with MIT's Nanostructures Laboratory. The HETG has 336 2.5-cm (1.0-in)-square grating facets. Microlithographic fabrication with laser interference patterns is used to produce the facets, which consist of gold grating bars with 50% filling factor on a polyimide substrate. The High Energy Gratings use gratings with two different periods that are oriented toward slightly different dispersion directions, forming a shallow "X" image on the readout detector. The medium-energy gratings (MEG) have 0.40-μm-thick gold bars on 0.50-μm-thick polyimide with 4000-Å period producing 2.85 Å/mm dispersion, and are placed behind the outer two AXAF mirrors. The High Energy Gratings, placed behind the inner two AXAF mirrors, are 0.70-μm-thick-gold bars on 1.0-μm-thick polyimide with 2000-Å period resulting in 5.7 Å/mm dispersion. The ACIS-S is the primary readout for the HETG.

The expected spectroscopic performance of AXAF, to be calibrated at the end of this year at Marshall Space Flight Center's x-ray Calibration Facility, is summarized in Figure 6.

Science with AXAF

Given the superb capabilities of the optics and associated instrumentation, the scientific possibilities of AXAF are nearly infinite. The most exciting investigations probably will result from the unexpected discoveries that improved sensitivity produces. AXAF will provide better angular resolution by about a factor of 10, and several orders of magnitude better spectroscopic resolution than previous x-ray astronomical observatories.

The determination and location of mass in the universe is a field of current interest. Observations with AXAF will be particularly well suited for measurement of the distribution of matter—the so-called "dark matter" (dark because we don't see it—yet we know that it is there)—on a variety of astronomical spatial scales including galaxies and clusters of galaxies. We know, for example, that the total mass in galaxy clusters is larger than the mass inferred from the luminous stars in the clusters. We also know, from previous x-ray observations, that the clusters are filled with an extremely hot x-ray-emitting gas. The mass in the gas does not account for the total mass, which clearly holds the cluster together through gravity. On the other hand, the hot x-ray-emitting gas serves as an ideal tracer to map the mass (strictly speaking, the gravitational potential). AXAF is ideal for this type of research. One needs large effective areas at energies well above the >2 keV temperatures characteristic of galaxy clusters, a reasonable field of view since even the more distant clusters are many arcminutes in size, and low scattering to obtain meaningful maps in regions of low surface brightness away from the cluster cores. Similar requirements are necessary to perform similar studies of individual galaxies, where the superb angular resolution comes into play.

Observations of the hot gas in galaxy clusters may also be used, in conjunction with ground-based radio measurements, to determine the distance to clusters and hence the Hubble constant. The approach, the Sunyaev-Zel'dovich effect, relates observations of the x-ray emitting gas with AXAF and the shift in frequency of the 3° (K) microwave background photons (relic of the big bang theory) occurring during scattering of energetic electrons. This combination of data determine the distance to the cluster, and thus the Hubble constant. Furthermore, after observations are made of several clusters at different distances, one can provide a possibly unambiguous measure of the age of the universe.

The concept that normal stars would be detectable as x-ray sources came decades ago with the recognition that our Sun possessed an "outer skin"—the solar corona—at very high, x-ray-emitting temperatures of several million degrees. The forerunners of AXAF, especially the Einstein Observatory and ROSAT, proved this conjecture correct and x-ray emission has been detected from practically all classes of normal stars (although in many cases the theorists are hard pressed to explain how the emission occurs!). AXAF, especially because of its capability for performing high-resolution spectroscopy, will provide a quantum leap in observational capability to measure coronal plasma parameters that are critical to our understanding of stellar coronae and comparison with our own sun.

AXAF will profoundly influence astronomy and astrophysics. The Observatory will be open for use by those scientists throughout the world who propose specific investigations. Data will be available through the AXAF Science Center, directed by H. Tannabaum, located at the SAO. The technical developments we describe are already an indication of the excitement to follow.

Martin C. Weisskopf is chief scientist for x-ray Astronomy and AXAF project scientist at NASA, Marshall Space Flight Center, Marshall Space Flight Center, Alabama, and Leon Van Speybroeck is senior research scientist and AXAF telescope scientist at Smithsonian Astrophysical Observatory, Cambridge, Mass.